ACS APPLIED POLYMER MATERIALS

pubs.acs.org/acsapm Article

Tuning the Properties of Surface-Anchored Polymer Networks by Varying the Concentration of a Thermally Activated Cross-Linker, Annealing Time, and Temperature in a One-Pot Reaction

Sun Young Woo, C. K. Pandiyarajan, and Jan Genzer*

Cite This: *ACS Appl. Polym. Mater.* 2021, 3, 5568−5577 Read Online

ACCESS | Metrics & More | Article Recommendations | Supporting Information

ABSTRACT: We investigate the properties of surface-anchored polymer networks created via one-pot synthesis using thermally active 6-azidosulfonylhexyltriethoxysilane (6-ASHTES). 6-ASHTES is a bifunctional gelator that undergoes cross-linking and surface-anchoring reactions when annealed above 100 °C. We employ a poly(vinylpyrrolidone) (PVP) with different molecular weights (10−1300 kDa) as a model system to examine the effect of 6-ASHTES concentration, annealing time, and annealing temperature on gel formation. A thin film of PVP/6-ASHTES mixture is deposited on a clean silicon wafer and annealed to form network layers. Spectroscopic ellipsometry measures the film thickness of the cross-linked layers from which the gel fraction and swelling ratio are determined. The gel fraction of PVP in the network can be "dialed in" by varying the annealing time, temperature, and concentration of 6-ASHTES in the PVP/6-ASHTES mixture. We use a simple Monte Carlo simulation model to describe cross-linking as a function of cross-linker concentration, reaction rate, reaction time, and polymer length. The trends obtained from the model simulations are in qualitative agreement with the experimental data.

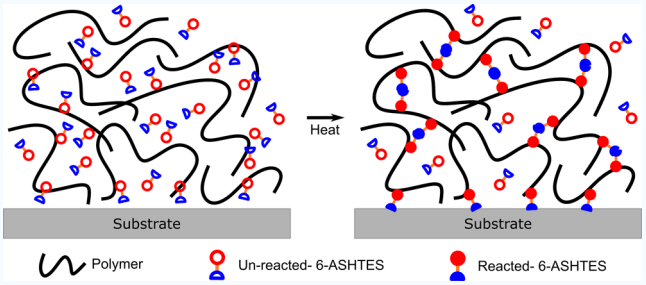

KEYWORDS: *hydrogel, substrate-anchored network, gel fraction, one-pot reaction, poly(vinylpyrrolidone), sulfonylazide, 6-ASHTES*

INTRODUCTION

Surface-anchored polymer networks have emerged as an exciting field of research due to their wide range of applications in coatings industries.[1−6] For example, neutral hydrophilic[7] or zwitterionic[8,9] polymer network films have gained enormous attention in antibiofouling[10−15] applications due to their swelling in aqueous media. Numerous methods have synthesized polymer brushes via "grafting to",[16] "grafting from",[17] and "grafting through"[18] methods. Typically, surface-anchored polymer chains or polymer brushes bear reactive functional units[19] and can be cross-linked with a difunctional molecule (di-thiols or di-hydro silanes), resulting in surface-anchored network layers.[19,20] Alternatively, a precursor homopolymer or copolymer comprising cross-linkable functionality can be deposited onto a solid substrate, which is then exposed to UV light or annealing, resulting in network formation.[21]

Prucker et al. have recently revealed a wide range of UV- and thermally active cross-linkers leading to the network formation via C−H insertion cross-linking (CHiC) reaction mechanism.[22−24] Accordingly, a precursor copolymer comprising UV-active methacryloyloxybenzophenone (MABP) is deposited on the silicon or a glass substrate precoated with a monolayer of benzophenone-containing silanes.[25] Upon UV irradiation, the benzophenone units present in the polymer and substrate are activated, triggering simultaneous cross-linking and surface-attachment reactions, thus creating surface-attached networks. Similar network layers can also be made by thermal means using styrene sulfonyl azides (SSAz).[26] Such techniques offer the ability to tune the network properties such as cross-link density, swelling, and elastic modulus of the networks in a gradient manner. However, the method involves the complex multistep synthesis of cross-linkers, surface-anchors, and copolymers, limiting their utility.

We recently developed a one-pot, one-step synthesis of surface-anchored network coatings using small bifunctional gelators (SBG) such as 6-azidosulfonylhexyltriethoxysilanes (6-ASHTES)[27] and 4-azidosulfonylphenethyltrimethoxysilane (4-ASPTMS).[28] The presence of sulfonylazide and alkoxysilanes enables the SBGs to undergo cross-linking and surface-attachment reactions simultaneously. These SBGs are commercially available and work with any common polymers and substrates as long as they contain C−H and/or −OH bonds in their structures. Our previous report explored the

Received: July 21, 2021
Accepted: September 22, 2021
Published: October 11, 2021

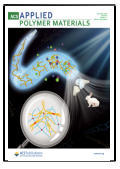

https://doi.org/10.1021/acsapm.1c00890
ACS Appl. Polym. Mater. 2021, 3, 5568−5577

effect of temperature, concentration of SBGs, and molecular structure of the polymers on gel formation. It allowed us to dial in a specific gel fraction of poly(vinylpyrrolidone) (PVP)/SBGs layer by adjusting temperature or concentration for a given time.

This work investigates the influence of the annealing time explicitly, the molecular weight of the polymer [i.e., poly(vinylpyrrolidone) (PVP)], and the ratio of 6-ASHTES to PVP on gel formation. We employ spectroscopic ellipsometry to measure the film thickness, from which we calculate the gel fraction and swelling ratios. In addition, we use a simple Monte Carlo model to understand the gelation of PVP/6-ASHTES layers and compare it qualitatively with experimental results. We note a consistent gelation trend with simulation and experimental results and find that the molecular weight of the precursor polymer (i.e., PVP) plays a critical role in the degree of cross-linking or gel fraction and has a significant effect on gel structure, e.g., swelling.

EXPERIMENTAL SECTION

Materials. 6-Azidosulfonylhexyltriethoxysilane (6-ASHTES) was purchased from Gelest (Morrisville, PA). Poly(vinylpyrrolidone) (PVP) was acquired from Sigma-Aldrich (St. Louis, MO) and used without purification. All solvents were purchased from Fisher Scientific (Pittsburgh, PA). Swelling experiments were performed using deionized (DI) water from the Milli-Q purification system with 10−15 MΩ·cm product resistivity. Silicon wafer (orientation ⟨100⟩, thickness 0.5 mm, and diameter 100 mm) was purchased from Silicon Valley Microelectronics (Santa Clara, CA).

Preparation of Surface-Anchored Networks. Polymer solutions were prepared with various ratios of 6-ASHTES and PVP in methanol (the weight fraction of 6-ASHTES in the solutions ranged from 1.3 to 20 wt %). First, a clean silicon wafer was exposed to ultraviolet/ozone (UVO) treatment for 5 min. A layer of PVP/6-ASHTES was then deposited using a dip coater (KSV NIMA single-vessel dip coater) at a 50−100 mm/min speed. Subsequently, the sample was placed on a hot stage (FP82HT, Mettler Toledo) and annealed at 120−140 °C allowing the layers to undergo cross-linking and surface-attachment reactions. Limited PVP diffusion would occur under those conditions because the annealing occurred below the glass-transition temperature of PVP (180 °C),[29] although 6-ASHTES may act as a plasticizer. We note that 6-ASHTES/6-ASHTES reactions may also occur. However, we cannot distinguish those from 6-ASHTES/PVP reactions. After annealing, the sample was cooled to room temperature and then extracted in methanol for 2 days, removing any unreacted or unbound materials from the silicon substrate. The initial dry thickness of the samples is ca. 60−180 nm.

Calculating Gel Fraction. We used spectroscopic ellipsometry to measure film thickness, from which we calculated the gel fraction (P_{gel}) according to eq 1.[28] The reflectivity scans were attained at a 70° angle of incidence (relative to the normal direction) in the spectral range of 400−800 nm in 60 steps (10 nm/step). These reflectivity scans were modeled using Fresnel formalism comprising a three-layer model in WVASE32 software (J.A. Woollam Co.). Layer 1: Si substrate layer 2: SiO_2 (1.5 nm thick); layer 3: polymer adlayer (Cauchy layer, $n = A_n + B_n/\lambda^2$, where n is the refractive index and A_n (=1.45−1.52) and B_n (=0.01 μm^2) are fitting parameters).

The Swelling Ratio of Surface-Attached Networks. The swelling of the network coatings was determined by measuring wet (or swollen) and dry (under ambient condition) layer thickness using spectroscopic ellipsometry equipped with a liquid cell. The sample containing PVP/6-ASHTES network film was immersed in a liquid cell filled with 100 mL of DI water and allowed to reach equilibrium (at least 10 min). All reflectivity scans were collected at a 70° (angle of incidence) from 400 to 800 nm spectral range. The swollen film thickness ($d^{solvent}$) was derived using an effective medium approximation (EMA).[30] The swelling ratio was then calculated from the ratio of swollen and dry thicknesses using eq 2.

RESULTS AND DISCUSSION

We investigated the formation of surface-attached network coatings using a simple one-pot synthesis using PVP with various molecular weights mixed with 6-ASHTES. First, we dissolved PVP and 6-ASHTES in methanol in multiple ratios and deposited a thin layer (∼100 nm) on a silicon wafer. Subsequently, the films were annealed at 120, 130, and 140 °C at various times and extracted in methanol. Figure S1 depicts morphologies of 6-ASHTES/PVP films with various 6-ASHTES wt % after annealing at 140 °C for 5 h and extraction in methanol. We described the cross-linking mechanism in our previous publication.[27] Upon annealing, the sulfonylazide in 6-ASHTES is activated and undergoes a C−H insertion, cross-linking reaction with neighboring polymer chains. Simultaneously, the triethoxysilane head groups enable self-condensation and condensation with the substrate hydroxy groups. Thus, the process produces surface-anchored polymer networks (Figure 1).

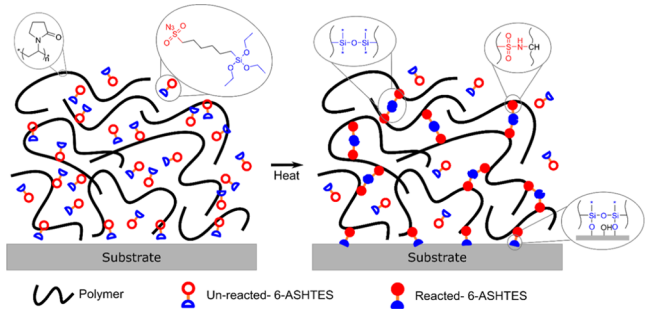

Figure 1. Generation of surface-attached PVP networks using 6-ASHTES, where the red circle and blue semicircle represent the sulfonylazide and triethoxy groups in 6-ASHTES. The open and solid symbols denote the reacted and unreacted 6-ASHTES molecules.

We monitored the kinetics of polymer film cross-linking on the substrate as a function of annealing time, annealing temperature, 6-ASHTES concentration, and molecular weight of PVP. We calculated the gel fraction (P_{gel}) from the change in film thickness before (d_0) and after (d) solvent extraction of the cross-linked polymer film

$$P_{gel} = \frac{d}{d_0} \quad (1)$$

For instance, $P_{gel} = 1$ indicates a network where all precursor polymers on the substrate have been incorporated into the gel. The samples had an initial thickness of ca. 60−180 nm. We note that the initial thickness of the polymer network does not have a significant effect on gel formation.

In Figure 2a, we plot the P_{gel} of the polymer network as a function of annealing time at 140 °C for the different molecular weights of PVP and fraction of 6-ASHTES in the gel. The molar ratio of PVP is 0.01 (open symbols) and 0.02 (closed symbols). The data shows that P_{gel} increases with increasing concentration of 6-ASHTES in the 6-ASHTES/PVP mixture and annealing time. Not surprisingly, the cross-linking reaction proceeds faster and to greater extents with reducing the PVP molecular weight. In Figure 2b, we plot P_{gel} as a function of the ratio of 6-ASHTES and VP repeat units

https://doi.org/10.1021/acsapm.1c00890
ACS Appl. Polym. Mater. 2021, 3, 5568−5577

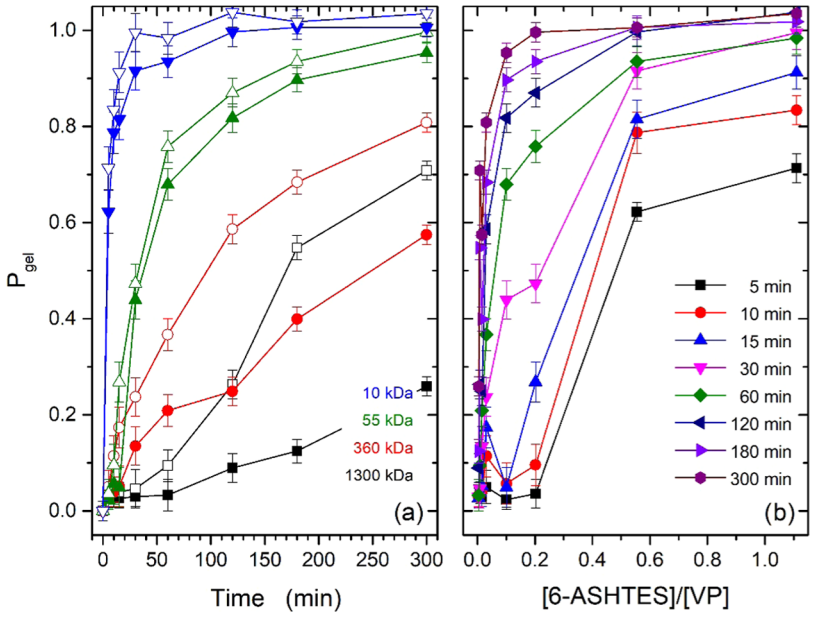

Figure 2. (a) Gel fraction (P_{gel}) of PVP networks as a function of various annealing times. The gels formed by cross-linking PVP having different molecular weights with 6-ASHTES at 140 °C. The open and closed symbols correspond to 0.01 and 0.02 mole fractions of PVP in 6-ASHTES/PVP films. (b) Gel fraction of PVP network from the left figure replotted as a function of the molar ratio of the 6-ASHTES and the total monomer for different annealing times. [] indicates a molar concentration of a given species.

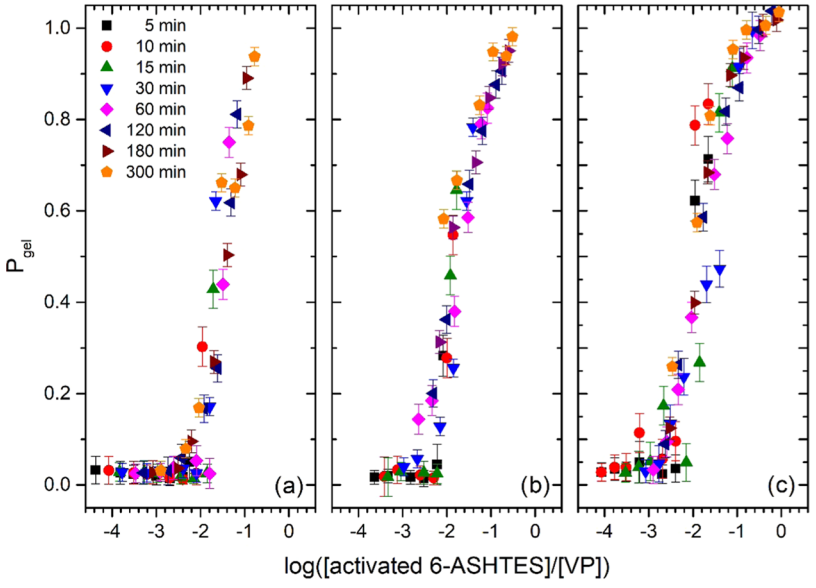

Figure 3. Gel fraction (P_{gel}) in PVP networks as a function of the logarithm of the molar ratio of the 6-ASHTES and VP units. The gels were formed by cross-linking PVP of different molecular weights and weight fractions of 6-ASHTES in PVP/6-ASHTES films for various annealing times at (a) 120 °C, (b) 130 °C, and (c) 140 °C. The different colors represent different gelation times. [] indicates a molar concentration of a given species.

concentration (i.e., monomers). Consistently, Figure 2b indicates that P_{gel} depends on the concentration of 6-ASHTES at the given time. In other words, one can prepare gels with the same value of P_{gel} by adjusting the amount of 6-ASHTES in the 6-ASHTES/PVP solution and annealing time. In previous studies,[27] P_{gel} of the PVP network rapidly increased by raising the annealing temperature from 100 to 140 °C.

It means that P_{gel} is controlled primarily by the thermal activation of the sulfonylazide groups. These results are consistent with the current data, as shown in Figure 3. We replot the data of Figure 2b as a function of the logarithm of 6-ASHTES and VP repeat unit ratio and shift the data horizontally using a shift factor (F^*) to produce a master plot presented in Figure 3c. In the abscissa, in Figure 3, log([activated 6-ASHTES]/[VP]) = log([6-ASHTES]/[VP]) + log(F^*). We repeated the above experiments with temperatures 120 and 130 °C (Figure 3a,b). The 6-ASHTES cross-links slowly at 120 °C compared with the higher temperatures at the given time and forms gels with a low P_{gel}. The P_{gel} value of the surface-anchored network can be adjusted by varying the concentration of the 6-ASHTES of polymer/cross-linker

https://doi.org/10.1021/acsapm.1c00890
ACS Appl. Polym. Mater. 2021, 3, 5568−5577

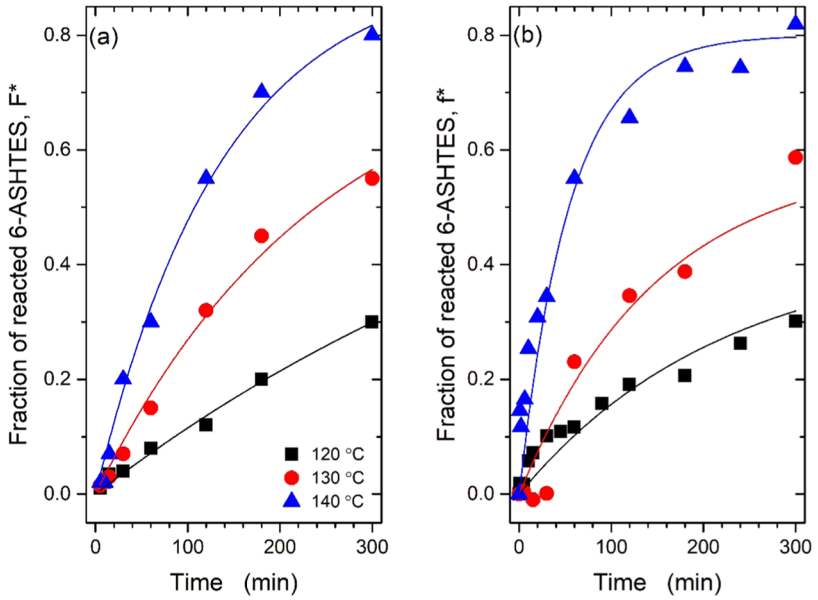

Figure 4. Fraction of reacted 6-ASHTES (F^* and f^*) as a function of annealing time at 120 °C (black), 130 °C (red), and 140 °C (blue). The weight fraction of 6-ASHTES was 10%. (a) F^* was obtained by shifting the data sets in Figure 2b horizontally. (b) f^* was obtained from ATR-FTIR spectra collected from PVP/6-ASHTES samples. The concentration of [activated 6-ASHTES] = F^* [6-ASHTES] or [activated 6-ASHTES] = f^* [6-ASHTES].

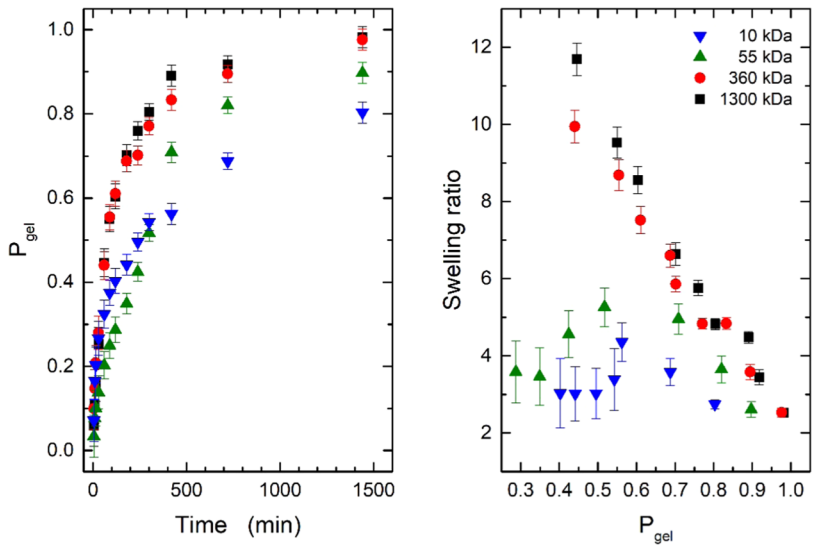

Figure 5. Gel fraction of PVP networks as a function of annealing time (left) and swelling ratio (right) of PVP network as a function of P_{gel}. All samples contained 10 wt % 6-ASHTES and were cross-linked by annealing at 140 °C.

mixture, annealing time, and annealing temperature independently.

The shift factors, F^*, needed to produce the master curves in Figure 3 are plotted in Figure 4a. The shift factor F^* represents the fraction of reacted 6-ASHTES groups during the cross-linking reaction. We also used attenuated total reflection-Fourier transform infrared spectroscopy (ATR-FTIR) to monitor the disappearance of the sulfonylazide group inside the polymer film and calculated the fraction of activated 6-ASHTES groups. We integrated the peak corresponding to the azide group (at vibration frequencies 2120−2160 cm^{-1}) and normalized the peak relative to the signal obtained from the same mixture before annealing (see the Supporting Information (SI) for details). The results for f^* were obtained from the FTIR analysis (see the SI and ref 25) are plotted in Figure 4b. The shifted data (Figure 4a) and the fraction of the activated azide (Figure 4b) were both fitted to first-order reaction kinetics that describes the concentration of 6-ASHTES before and after the reaction (see eq S3 in the SI).

Using the ATR-FTIR data, we monitored the consumption of the sulfonylazide groups. In the kinetic model (see the SI), we assumed that this process translated directly to the formation of sulfonyl amide linkers. We admit that this may not be the case. We do not have means of monitoring the concentration of sulfonyl amide bonds. We also assumed that the siloxane bonds cross-linked faster than the reaction involving sulfonyl groups. We provided evidence of this in our previous paper.[27] However, the high reactivity of siloxane bonds may result in clusters involving more than just two 6-ASHTES molecules. Hence, the fraction of reacted 6-ASHTES

https://doi.org/10.1021/acsapm.1c00890
ACS Appl. Polym. Mater. 2021, 3, 5568−5577

may not represent the actual density of the cross-linking points. The fractions of reacted 6-ASHTES obtained by shifting the P_{gel} data sets (cf. F^* in Figure 4a) and those extracted from FTIR-ATR analysis (cf. f^* in Figure 4b) exhibit a similar dependence on annealing time and activation energy (cf. Figure S3 and Table S1). This observation gives us confidence that the number of silane molecules in the condensed clusters does not vary among experiments.

We made samples containing 10 wt % of 6-ASHTES with various PVP molecular weights to investigate the surface-attached network swelling behavior in deionized water. All samples were annealed between 5 and 1440 min at 140 °C. The gel fractions of samples are plotted in Figure 5a. P_{gel} of the two highest PVP molecular weights (i.e., 360 and 1300 kDa) increase considerably with increasing time and reach a plateau, indicating final cross-linking. However, 10 and 55 kDa PVP layers do not show a plateau in 1440 min annealing time.

We define the swelling ratio, $\alpha^{solvent}$, of the polymer network by eq 2

$$\alpha^{solvent} = \frac{d^{solvent}}{d} \tag{2}$$

where d is the dry thickness of PVP and $d^{solvent}$ is the thickness of the same polymer layer after swelling in water. The swelling ratio increases with decreasing P_{gel}, as expected (cf. Figure 5b). At a high P_{gel} (>0.7−0.8), the swelling ratio has the same dependence on P_{gel} for all molecular weights increasing with decreasing gel fraction. However, at a low P_{gel} (<0.7), the swelling ratio of 10 and 55 kDa samples deviates from this trend. We further support this trend by plotting P_{gel} (cf. Figure 6) and the swelling ratio (cf. Figure 7) from gels prepared by cross-linking PVP of various molecular weights with 6-ASHTES with concentrations ranging from 5 to 20 wt %.

Figure 6 plots the corresponding P_{gel} dependence on cross-linking time. Gels made of a higher-molecular-weight PVP (360 and 1300 kDa) and a higher weight fraction of 6-ASHTES exhibit a steady increase in P_{gel} independent of the

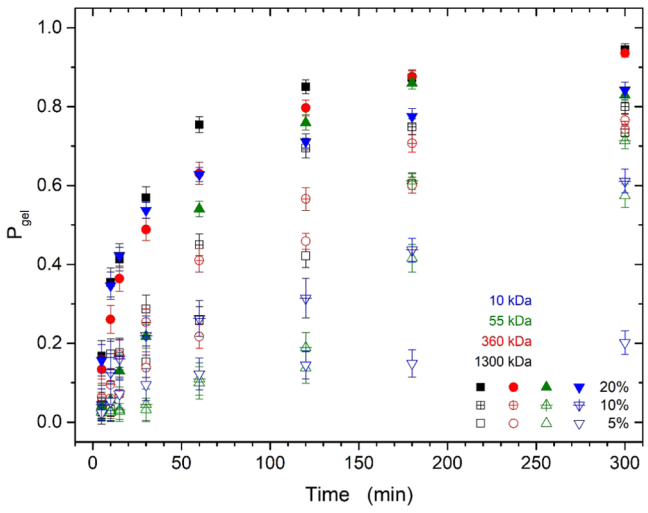

Figure 6. Gel fraction (P_{gel}) of PVP networks prepared by reacting PVP of various molecular weights and PVP/6-ASHTES concentrations at 140 °C multiple times. The different colors represent different molecular weights of PVP. Open, crossed, and closed symbols correspond to the weight percent of 6-ASHTES in the 6-ASHTES/PVP mixture ranging from 5 to 20%.

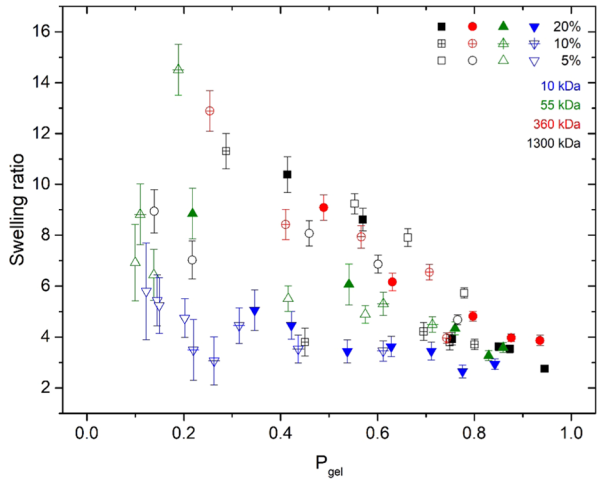

Figure 7. Swelling ratio of PVP networks prepared by reacting PVP of various molecular weights and PVP/6-ASHTES concentrations at 140 °C at different times. The different colors represent different molecular weights of PVP. Open, crossed, and closed symbols correspond to the weight percent of 6-ASHTES in the 6-ASHTES/PVP mixture ranging from 5 to 20%.

molecular weight of PVP. However, gels prepared from a low-molecular-weight PVP (10 and 55 kDa) and a lower weight fraction of 6-ASHTES feature a larger scatter in P_{gel} as a function of annealing time. Figure 7 displays the swelling ratios of the gels formed by cross-linking PVP of various molecular weights with 6-ASHTES with concentrations ranging from 5 to 20 wt %. As in Figure 5b, the swelling ratio for PVP polymers with a high molecular weight and a high concentration of 6-ASHTES increases steadily with decreasing P_{gel}. However, the swelling ratio in gels prepared from a lower-molecular-weight PVP or a lower concentration of 6-ASHTES does not increase considerably with decreasing P_{gel}. Later in this paper, we present the results of a simple computer simulation model, which demonstrates that P_{gel} increases with reaction time and attains the same value for polymers cross-linked with the same weight fraction of the cross-linker, regardless of the molecular weight of the polymer. We attribute the behavior described in the data in Figures 6 and 7 to imperfect gels with heterogeneities in their structure. Ellipsometry measures the average thickness of the swollen film. It cannot detect local inhomogeneities in the film structure. Therefore, one needs to consider measuring both P_{gel} and the swelling ratio to characterize the gel structure fully. We conclude that shorter polymers cannot form homogeneous, uniformly cross-linked networks.

We developed a simple Monte Carlo kinetic model that describes cross-linking in our system (see the SI for more information). We use the model to confirm the scaling we employed in interpreting the experimental data and provide more insight into the effect of the molecular weight of polymers on gel properties. We provide the details of the model in the SI.

In Figure 8, we plot the gel fraction (P_{gel}) as a function of the Monte Carlo steps (MCS) while varying the ratio of the concentration of the cross-linker ([X]) to monomer (Figure 8a) and the rate constant (k) while keeping the concentration of monomers ([M]) the same. Overall, P_{gel} increases with increasing the [X]/[M] ratio and increasing k. Increasing the reaction time (MCS in computer simulations) further

https://doi.org/10.1021/acsapm.1c00890
ACS Appl. Polym. Mater. 2021, 3, 5568−5577

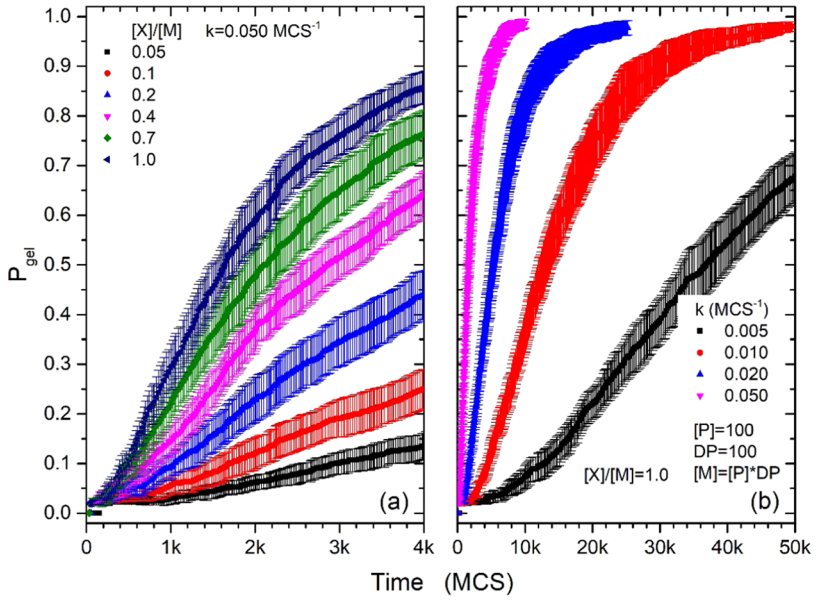

Figure 8. Gel fraction of gels (P_{gel}) as a function of Monte Carlo steps (MCS), equivalent to time. (a) P_{gel} for various ratios of cross-linker ([X]) and monomer ([M]) and constant reaction rate (k), number of polymers, and degree of polymerization (DP). P_{gel} increases with increasing [X]/[M]. (b) P_{gel} for values of k and constant [X]/[M] and a constant number of polymer and degree of polymerization. P_{gel} increases with increasing k.

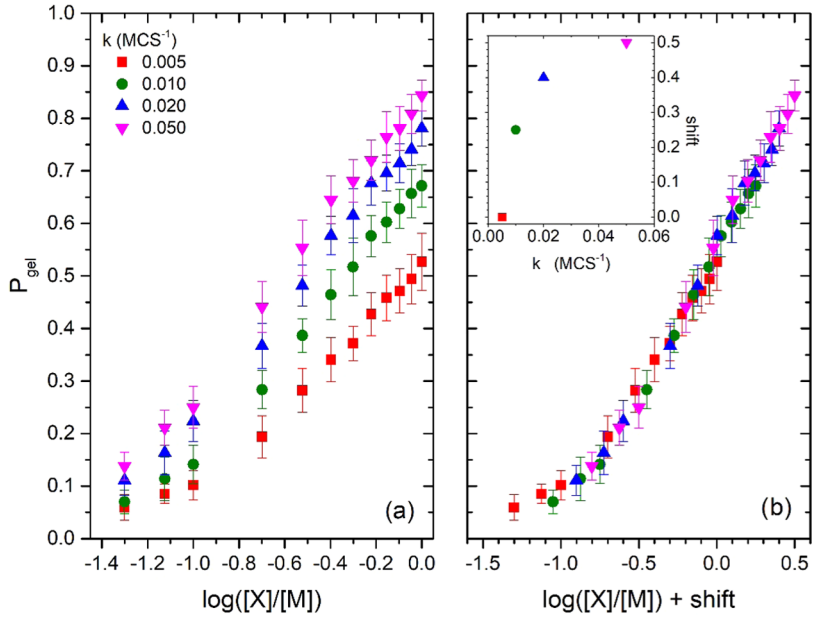

Figure 9. (a) Gel fraction of gels (P_{gel}) as a function of log([X]/[M]) for various reaction rates (k) and a fixed number of polymers and degree of polymerization after 200 Monte Carlo steps. (b) Same data as in (a), except that the abscissa has been replotted as log([X]/[M]) + shift. The values of the shift factor as a function of k are displayed in the inset to (b).

promotes the two trends. We have verified that these trends hold for other [X]/[M] ratios and a different number of polymers and different degrees of polymerizations. The results are in qualitative agreement with the trends in our experimental data, which reveal that P_{gel} increases with increasing the cross-linker concentration in polymer/cross-linker mixture and increasing the reaction temperature. In the simulations and experimental data, we detect that P_{gel} follows a sigmoidal trend with time (or MCS). It initially increases gradually, then the rate of P_{gel} rise increases, and finally, it levels off at longer times (or MCS).

In Figure 9a, we plot P_{gel} as a function of the cross-linker concentration [X] and the monomer concentrations [M] for different temperatures (i.e., k values) after 200 MCS. We plot P_{gel} as a function of the log of [X]/[M]. Increasing the temperature (or k) gives rise to a higher value of P_{gel} for a given value of log([X]/[M]). This behavior is understandable as the cross-linking rate and P_{gel} increase with increasing temperature (or k). Figure 9b plots the data from Figure 9a by shifting the abscissa by a given amount (i.e., shift) to produce master plots. We plot the "shift" values as a function of k in the inset to Figure 9b. The physical meaning of shift can be understood as a correction to the number of cross-linkers activated to participate in cross-linking. Hence, log([X]/[M]) + shift can be written as $\log(10^{shift}[X]/[M])$, where $10^{shift}[X]$ is the number of activated cross-linkers.

https://doi.org/10.1021/acsapm.1c00890
ACS Appl. Polym. Mater. 2021, 3, 5568−5577

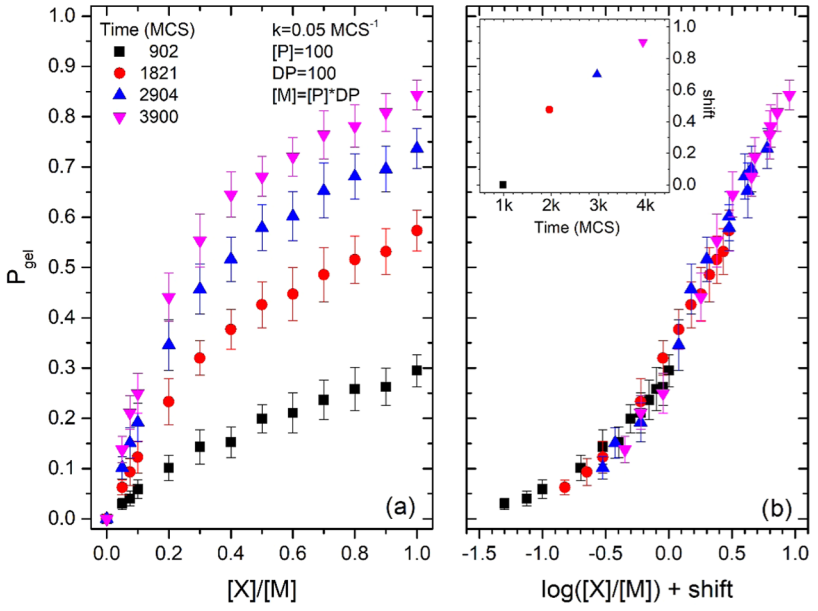

Figure 10. (a) Gel fraction of gels (P_{gel}) as a function of log([X]/[M]) for various reaction MCS for a fixed value of k and a fixed number of polymers and degree of polymerization (DP) after 200 MCS. (b) Same data as in (a), except that the abscissa has been replotted as log([X]/[M]) + shift. The values of the shift factor as a function of MCS are displayed in the inset to (b).

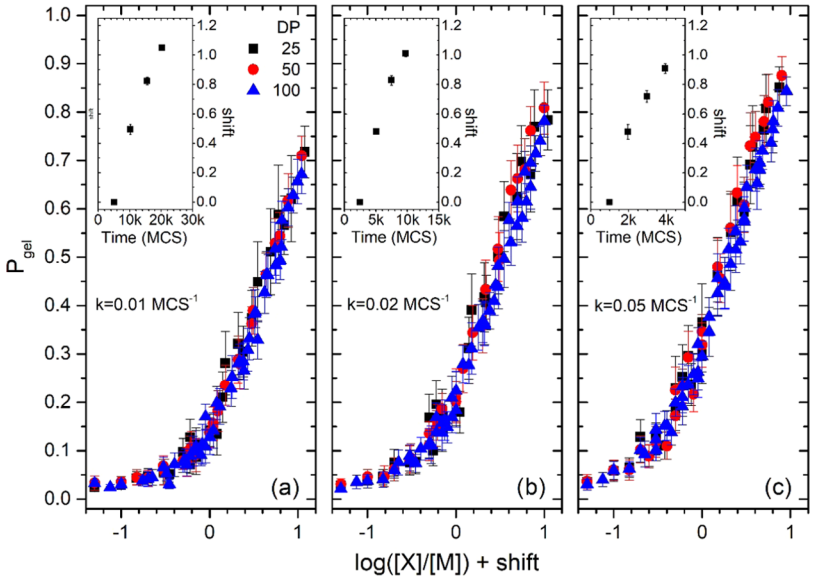

Figure 11. (a) Gel fraction of gels (P_{gel}) as a function of log([X]/[M]) + shift for various degrees of polymerization (DP) and three different rate constants: (a) k = 0.01, (b) k = 0.02, and (c) k = 0.05. The values of the shift factor as a function of MCS are displayed in the insets to (a−c).

Figure 10a plots P_{gel} as a function of the [X]/[M] ratio from different MCS while keeping k, the number of polymers, and their degree of polymerization constant. P_{gel} increases with increasing [X]/[M] and increasing the polymerization time (or MCS). This behavior is consistent for all numbers of polymers and degrees of polymerization. Figure 10b plots the data from Figure 10a by shifting the abscissa by a given amount (i.e., shift) to produce master plots. The values of shift as a function of MCS are plotted in the inset to Figure 10b. The physical meaning of shift can be understood as a correction to the number of cross-linkers activated to participate in cross-linking. As noted previously, log([X]/[M])+shift can be written as log(10^{shift}[X]/[M]), where 10^{shift}[X] denotes the number of activated cross-linkers.

In Figure 11, we plot P_{gel} as a function log([X]/[M])+shift for cross-linking reaction performed with polymers having three different degrees of polymerization (25, 50, 100) at three different temperatures (or k), equal to: (a) k = 0.01, (b) k = 0.02, and (c) k = 0.05. The values of shift as a function of MCS are plotted in the insets to Figure 11a−c. The physical meaning of shift remains the same; i.e., log([X]/[M]) + shift can be written as log(10^{shift}[X]/[M]), where 10^{shift}[X] is the number of activated cross-linkers.

Finally, we return to the discussion of gel properties as a function of the molecular weight of the parent polymers. In Figure 12, we plot P_{gel} as a function of reaction time for k = 0.01 MCS^{-1} and polymers having different molecular weights. We plot the data for three [X]/[M] ratios; the complete data

https://doi.org/10.1021/acsapm.1c00890
ACS Appl. Polym. Mater. 2021, 3, 5568−5577

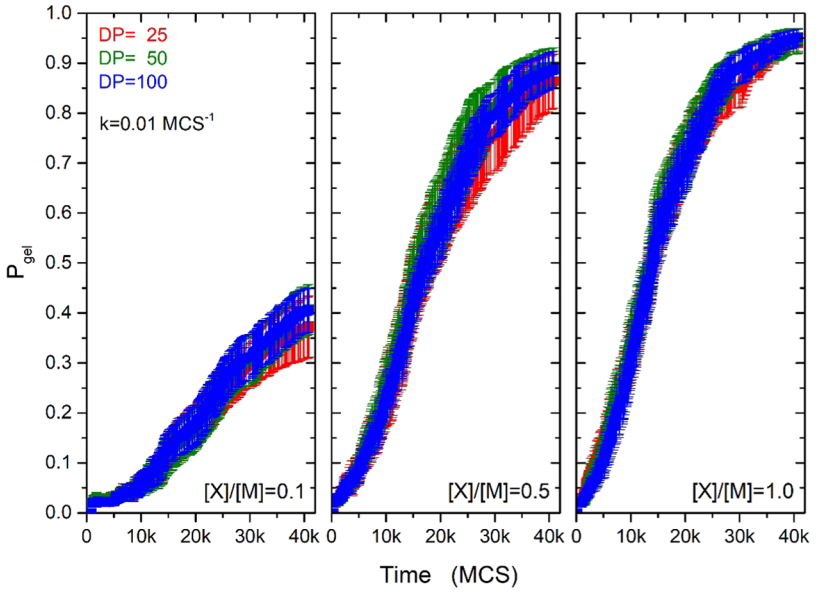

Figure 12. Gel fraction of gels (P_{gel}) as a function of time at various degrees of polymerization (DP). We used k = 0.01 and varied the cross-linker/monomer ratio [X]/[M] from 0.1 to 0.5 and 1.0.

set featuring four different k values and six [X]/[M] values are shown in the SI. The data in Figure 12 show that, for a given [X]/[M] ratio, P_{gel} exhibits universal dependence on time. To connect $[n_{6\text{-ASHTES}}]/[VP]$ to the weight fraction of 6-ASHTES, we write

$$w_X = \frac{m_X}{m_X + m_M} = \frac{[X]M_X}{[X]M_X + [M]M_M} = \frac{\frac{[X]}{[M]}M_X}{\frac{[X]}{[M]}M_X + M_M} \quad (3)$$

After some algebra, eq 3 reduces to

$$\frac{[X]}{[M]} = \frac{M_M}{M_X}\left(\frac{w_X}{1 - w_X}\right) \quad (4)$$

$$\frac{[6 - ASHTES]}{[VP]} = \frac{M_{VP}}{M_{6-ASHTES}}\left(\frac{w_{6-ASHTES}}{1 - w_{6-ASHTES}}\right) = 0.314\left(\frac{w_{6-ASHTES}}{1 - w_{6-ASHTES}}\right) \quad (5)$$

We have previously determined that P_{gel} depends on the ratio of cross-linker and the number of cross-linkable units in the polymer. Regardless of the molecular weight, gels formed at a given weight fraction of the cross-linker should exhibit the same P_{gel}. The data shown in Figures 5−7 show that networks formed with a low-molecular-weight/low cross-linker density are imperfect.

We recognize that the model has limitations. It assumes that the polymers exist as rigid rods resting without motion on a two-dimensional (2D) lattice. We further consider that the cross-linkers featured bifunctional cross-linkers that link two neighboring chains. Despite these limitations, our results confirm that a specific value of P_{gel} can be "dialed in" by varying the concentration of the cross-linker (X), the annealing time (or MCS), and the annealing temperature (k) independently. We confirmed that a unique value of P_{gel} could be dialed in at a given log([X]/[M])+ shift. The physical meaning of the shift factor is 10^{shift}[X]; it represents the number of activated cross-linkers. We established the dependence of the shift factor on temperature, cross-linker concentration, and annealing time. Overall the simulation studies confirm the findings in our experimental studies.

CONCLUSIONS

In this work, we study the kinetics of formation of the surface-anchored poly(vinylpyrrolidone) (PVP) networks using a thermally active bifunctional cross-linker 6-azidosulfonylhexyltriethoxysilane (6-ASHTES), at various 6-ASHTES concentrations, PVP molecular weights, annealing temperatures, and annealing times. 6-ASHTES also acts as an anchoring agent that immobilizes the cross-linked PVP on the surface (although some PVP may attach to the substrate via H bonds). We evaluate the gel fraction (P_{gel}), i.e., the amount of polymer left on the substrate after cross-linking relative to the initial amount, and swelling ratio of the substrate-anchored gel in water using spectroscopic ellipsometry. We show that P_{gel} data collected from samples with various polymer/cross-linker ratios annealed at different temperatures and times can be collapsed onto universal master plots. This concentration−time−temperature superposition reveals that P_{gel} in the gel can be adjusted by tailoring the amounts of polymer and cross-linker, the reaction conditions, the annealing temperature, and the annealing time. We evaluate the activation energy for cross-linking from the shifting factor of the master curves and the disappearance of sulfonylazide as monitored by ATR-FTIR. We use swelling experiments to study the gel structure. While gels made of a high-molecular-weight PVP form uniform networks, gels prepared from a low-molecular-weight PVP and low concentrations of 6-ASHTES are heterogeneous. We also developed a simple Monte Carlo model that simulates the formation of cross-linked networks as a function of the concentration of the cross-linking agent, the molecular weight of the "polymer", and temperature. The simulation data can be collapsed on similar master curves as the experimental data. While we only report experimental data for PVP in this work, we have evidence that networks can be formed from other polymers as long as they contain C−H bonds. This result

https://doi.org/10.1021/acsapm.1c00890
ACS Appl. Polym. Mater. 2021, 3, 5568−5577

opens up possibilities for creating functional polymeric networks using commodity polymers without specialized chemical synthesis. This work may open the door to many potential applications, including (but not limited to) functional coatings, selective membranes, and many others.

■ ASSOCIATED CONTENT

Supporting Information

The Supporting Information is available free of charge at https://pubs.acs.org/doi/10.1021/acsapm.1c00890.

Image analysis of 6-ASHTES/PVP films; ATR-FTIR analysis of reaction kinetics; and Monte Carlo model of cross-linking reaction (PDF)

■ AUTHOR INFORMATION

Corresponding Author

Jan Genzer − *Department of Chemical & Biomolecular Engineering, North Carolina State University, Raleigh, North Carolina 27695-7905, United States; Global Station for Soft Matter, Global Institution for Collaborative Research and Education (GI-CoRE), Hokkaido University, Hokkaido 060-0808, Japan;* orcid.org/0000-0002-1633-238X; Email: jgenzer@ncsu.edu

Authors

Sun Young Woo − *Department of Chemical & Biomolecular Engineering, North Carolina State University, Raleigh, North Carolina 27695-7905, United States*

C. K. Pandiyarajan − *Department of Chemical & Biomolecular Engineering, North Carolina State University, Raleigh, North Carolina 27695-7905, United States;* orcid.org/0000-0002-8954-9141

Complete contact information is available at: https://pubs.acs.org/10.1021/acsapm.1c00890

Notes

The authors declare no competing financial interest.

■ ACKNOWLEDGMENTS

This work was supported by a grant NSF DMR-1809453. Partial support from the S. Frank and Doris Culberson funds is appreciated. The authors thank Dr. Erik Santiso (NC State University) for fruitful discussions.

■ REFERENCES

(1) Carr, L. R.; Krause, J. E.; Ella-Menye, J. R.; Jiang, S. Single Nonfouling Hydrogels with Mechanical and Chemical Functionality Gradients. *Biomaterials* **2011**, *32*, 8456−8461.

(2) Zhang, L.; Cao, Z.; Bai, T.; Carr, L.; Ella-Menye, J.-R.; Irvin, C.; Ratner, B. D.; Jiang, S. Zwitterionic Hydrogels Implanted in Mice Resist the Foreign-Body Reaction. *Nat. Biotechnol.* **2013**, *31*, 553−556.

(3) Chen, S.; Zheng, J.; Li, L.; Jiang, S. Strong Resistance of Phosphorylcholine Self-Assembled Monolayers to Protein Adsorption: Insights into Nonfouling Properties of Zwitterionic Materials. *J. Am. Chem. Soc.* **2005**, *127*, 14473−14478.

(4) Shih, Y. J.; Chang, Y. Tunable Blood Compatibility of Polysulfobetaine from Controllable Molecular-Weight Dependence of Zwitterionic Nonfouling Nature in Aqueous Solution. *Langmuir* **2010**, *26*, 17286−17294.

(5) Huang, C. J.; Wang, L. C.; Shyue, J. J.; Chang, Y. C. Developing Antifouling Biointerfaces Based on Bioinspired Zwitterionic Dopamine through PH-Modulated Assembly. *Langmuir* **2014**, *30*, 12638−12646.

(6) Schlenoff, J. B. Zwitteration: Coating Surfaces with Zwitterionic Functionality to Reduce Nonspecific Adsorption. *Langmuir* **2014**, *30*, 9625−9636.

(7) Pandiyarajan, C. K.; Prucker, O.; Zieger, B.; Rühe, J. Influence of the Molecular Structure of Surface-Attached Poly(N-Alkyl Acrylamide) Coatings on the Interaction of Surfaces with Proteins, Cells and Blood Platelets. *Macromol. Biosci.* **2013**, *13*, 873−884.

(8) Zhang, L.; Cao, Z.; Bai, T.; Carr, L.; Ella-Menye, J.-R.; Irvin, C.; Ratner, B. D.; Jiang, S. Zwitterionic Hydrogels Implanted in Mice Resist the Foreign-Body Reaction. *Nat. Biotechnol.* **2013**, *31*, 553−556.

(9) Carr, L. R.; Xue, H.; Jiang, S. Functionalizable and Nonfouling Zwitterionic Carboxybetaine Hydrogels with a Carboxybetaine Dimethacrylate Crosslinker. *Biomaterials* **2011**, *32*, 961−968.

(10) Ventura, C.; Guerin, A. J.; El-Zubir, O.; Ruiz-Sanchez, A. J.; Dixon, L. I.; Reynolds, K. I.; Dale, M. L.; Ferguson, J.; Houlton, A.; Horrocks, B. R.; Clare, A. S.; Fulton, D. A. Marine Antifouling Performance of Polymer Coatings Incorporating Zwitterions. *Biofouling* **2017**, *33*, 892−903.

(11) Higaki, Y.; Kobayashi, M.; Murakami, D.; Takahara, A. Anti-Fouling Behavior of Polymer Brush Immobilized Surfaces. *Polym. J.* **2016**, *48*, 325−331.

(12) Leonardi, A. K.; Ober, C. K. Polymer-Based Marine Antifouling and Fouling Release Surfaces: Strategies for Synthesis and Modification. *Annu. Rev. Chem. Biomol. Eng.* **2019**, *10*, 241−264.

(13) Zhu, X.; Jańczewski, D.; Lee, S. S. C.; Teo, S. L.-M.; Vancso, G. J. Cross-Linked Polyelectrolyte Multilayers for Marine Antifouling Applications. *ACS Appl. Mater. Interfaces* **2013**, *5*, 5961−5968.

(14) Callow, J. A.; Callow, M. E. Trends in the Development of Environmentally Friendly Fouling-Resistant Marine Coatings. *Nat. Commun.* **2011**, *2*, No. 244.

(15) Bauer, S.; Arpa-Sancet, M. P.; Finlay, J. A.; Callow, M. E.; Callow, J. A.; Rosenhahn, A. Adhesion of Marine Fouling Organisms on Hydrophilic and Amphiphilic Polysaccharides. *Langmuir* **2013**, *29*, 4039−4047.

(16) *Polymer Brushes*; Brittain, W. J.; Advincula, R.; Caster, K. C.; Rühe, J., Eds.; Wiley-VCH Verlag GmbH & Co. KGaA: Weinheim, 2004.

(17) Zoppe, J. O.; Ataman, N. C.; Mocny, P.; Wang, J.; Moraes, J.; Klok, H. A. Surface-Initiated Controlled Radical Polymerization: State-of-the-Art, Opportunities, and Challenges in Surface and Interface Engineering with Polymer Brushes. *Chem. Rev.* **2017**, *117*, 1105−1318.

(18) Enright, T. P.; Hagaman, D.; Kokoruz, M.; Coleman, N.; Sidorenko, A. Gradient and Patterned Polymer Brushes by Photo-initiated "Grafting through" Approach. *J. Polym. Sci., Part B: Polym. Phys.* **2010**, *48*, 1616−1622.

(19) Chollet, B.; Li, M.; Martwong, E.; Bresson, B.; Fretigny, C. Multiscale Surface-Attached Hydrogel Thin Films with Tailored Architecture. *ACS Appl. Mater. Interfaces* **2016**, *8*, 11729−11738.

(20) Chollet, B.; Eramo, D.; Martwong, E.; Li, M.; Macron, J.; Mai, T. Q.; Tabeling, P.; Tran, Y.; Supe, E. Tailoring Patterns of Surface-Attached Multiresponsive Polymer Networks. *ACS Appl. Mater. Interfaces* **2016**, *8*, 24870−24879.

(21) Pandiyarajan, C. K.; Rubinstein, M.; Genzer, J. Surface-Anchored Poly(N -Isopropylacrylamide) Orthogonal Gradient Networks. *Macromolecules* **2016**, *49*, 5076−5083.

(22) Kost, J.; Bleiziffer, A.; Rusitov, D.; Rühe, J. Thermally Induced Cross-Linking of Polymers via C,H Insertion Cross-Linking (CHic) under Mild Conditions. *J. Am. Chem. Soc.* **2021**, *143*, 10108−10119.

(23) Prucker, O.; Brandstetter, T.; Rühe, J. Surface-Attached Hydrogel Coatings via C,H-Insertion Crosslinking for Biomedical and Bioanalytical Applications (Review). *Biointerphases* **2018**, *13*, No. 010801.

(24) Kanokwijitsilp, T.; Körner, M.; Prucker, O.; Anton, A.; Lübke, J.; Rühe, J. Kinetics of Photocrosslinking and Surface Attachment of Thick Polymer Films. *Macromolecules* **2021**, *54*, 6238−6246.

(25) Prucker, O.; Naumann, C. A.; Rühe, J.; Knoll, W.; Frank, C. W. Photochemical Attachment of Polymer Films to Solid Surfaces via

Monolayers of Benzophenone Derivatives. *J. Am. Chem. Soc.* **1999**, *121*, 8766−8770.
(26) Schuh, K.; Prucker, O.; Rühe, J. Surface Attached Polymer Networks through Thermally Induced Cross-Linking of Sulfonyl Azide Group Containing Polymers. *Macromolecules* **2008**, *41*, 9284−9289.
(27) Pandiyarajan, C. K.; Genzer, J. Thermally Activated One-Pot, Simultaneous Radical and Condensation Reactions Generate Surface-Anchored Network Layers from Common Polymers. *Macromolecules* **2019**, *52*, 700−707.
(28) Pandiyarajan, C. K.; Genzer, J. UV- and Thermally-Active Bi-Functional Gelators Create Surface-Anchored Polymer Networks. *Macromol. Rapid Commun.* **2021**, *42*, No. 2100266.
(29) Turner, D. T.; Schwartz, A. The Glass Transition Temperature of Poly(N-Vinyl Pyrrolidone) by Differential Scanning Calorimetry. *Polymer* **1985**, *26*, 757−762.
(30) Pandiyarajan, C. K.; Genzer, J. Effect of Network Density in Surface-Anchored Poly(N-Isopropylacrylamide) Hydrogels on Adsorption of Fibrinogen. *Langmuir* **2017**, *33*, 1974−1983.

https://doi.org/10.1021/acsapm.1c00890
ACS Appl. Polym. Mater. 2021, 3, 5568−5577